α-hederin overcomes hypoxia-mediated drug resistance in colorectal cancer by inhibiting the AKT/Bcl2 pathway

JINBAO CHEN[1*], JIAN XU[1*], JIAHUA YANG[2*], YUEPING ZHAN[1], SEN LI[2], LINLIN JIA[1], WENTAO WU[2], XIANKE SI[2], DIE ZHANG[1], KUN YU[2], PEIHAO YIN[1-3], YIJUN CAO[2], WANLI DENG[4], KE XU[5] and WEI LI[2,3]

[1]Interventional Cancer Institute of Chinese Integrative Medicine, Putuo Hospital, Shanghai University of Traditional Chinese Medicine; [2]Department of General Surgery, Putuo Hospital, Shanghai University of Traditional Chinese Medicine, Shanghai 200062; [3]Shanghai Putuo Central School of Clinical Medicine, Anhui Medicine University, Hefei, Anhui 230032; [4]Department of Medical Oncology, Putuo Hospital, Shanghai University of Traditional Chinese Medicine, Shanghai 200062; [5]Institute of Translational Medicine, Shanghai University, Shanghai 200444, P.R. China

Received June 3, 2022; Accepted December 29, 2022

DOI: 10.3892/ijo.2023.5481

Abstract. Currently, chemoresistance is a major challenge that directly affects the prognosis of patients with colorectal cancer (CRC). In addition, hypoxia is associated with poor prognosis and therapeutic resistance in patients with cancer. Accumulating evidence has shown that α-hederin has significant antitumour effects and that α-hederin can inhibit hypoxia-mediated drug resistance in CRC; however, the underlying mechanism remains unclear. In the present study, viability and proliferation assays were used to evaluate the effect of α-hederin on the drug resistance of CRC cells under hypoxia. Sequencing analysis and apoptosis assays were used to determine the effect of α-hederin on apoptosis under hypoxia. Western blot analysis and reverse transcription-quantitative PCR were used to measure apoptosis-related protein and mRNA expression levels. Furthermore, different mouse models were established to study the effect of α-hederin on hypoxia-mediated CRC drug resistance *in vivo*. In the present study, the high expression of Bcl2 in hypoxic CRC cells was revealed to be a key factor in their drug resistance, whereas α-hederin inhibited the expression of Bcl2 by reducing AKT phosphorylation *in vitro* and *in vivo*, and promoted the apoptosis of CRC cells under hypoxia. By contrast, overexpression of AKT reversed the effect of α-hederin on CRC cell apoptosis under hypoxia. Taken together, these results suggested that α-hederin may overcome hypoxia-mediated drug resistance in CRC by inhibiting the AKT/Bcl2 pathway. In the future, α-hederin may be used as a novel adjuvant for reversing drug resistance in CRC.

Correspondence to: Professor Wei Li, Department of General Surgery, Putuo Hospital, Shanghai University of Traditional Chinese Medicine, 164 Lanxi Road, Shanghai 200062, P.R. China
E-mail: liwei1825@shutcm.edu

Professor Ke Xu, Institute of Translational Medicine, Shanghai University, 99 Shangda Road, Shanghai 200444, P.R. China
E-mail: cola519@163.com

[*]Contributed equally

Abbreviations: CRC, colorectal cancer; OXA, oxaliplatin; 5-FU, 5-fluorouracil; CCK-8, Cell Counting Kit-8; IHC, immunohistochemistry; OE, overexpression; qPCR, quantitative PCR; WB, western blot

Key words: CRC, α-hederin, Bcl2, hypoxia, chemoresistance

Introduction

Currently, tumour cell resistance to chemotherapy is one of the leading causes of colorectal cancer (CRC)-related death (1). Therefore, a more comprehensive understanding of drug resistance mechanisms is required to better combat this disease.

It is well known that hypoxia is closely related to the occurrence and development of tumours, and is a common phenomenon in most malignant tumours (2). Hypoxia occurs during tumorigenesis because of insufficient oxygen supply due to irregularities or spacing of tumour blood vessels. Cancer cells survive mainly by adapting to the environment in response to hypoxia through a variety of cellular mechanisms (3). Hypoxia serves important roles in tumour initiation and progression, especially in promoting tumour chemotherapy resistance (4). The hypoxic microenvironment can promote chemoresistance in tumour cells through a variety of related mechanisms, including inhibition of apoptotic signalling pathways, which is one of the mechanisms that leads to tumour chemoresistance (5-7). In the hypoxic tumour microenvironment, the expression of Bcl2 increases, whereas that of proapoptotic proteins decreases, and tumour cells overexpressing Bcl2 can lead to drug resistance due to their decreased apoptotic ability (8). Thus, strategies that can regulate hypoxia-mediated drug resistance in CRC have broad clinical potential.

α-hederin is a typical pentacyclic triterpene saponin, and a large number of studies have shown that pentacyclic triterpene

saponins have a wide range of biological activities, such as antitumour, antiviral, anti-inflammatory and immunoregulatory activities (9). To date, extensive research has been carried out on the antitumour effects of α-hederin, such as inhibition of tumour cell metastasis and tumour immune evasion, and enhancement of chemotherapeutic drug sensitivity (10-14). Therefore, it was hypothesized that α-hederin may inhibit the expression of Bcl2 by reducing the phosphorylation of AKT, thereby overcoming hypoxia-mediated drug resistance in CRC. The present study explored the mechanism by which α-hederin overcomes hypoxia-mediated chemoresistance in CRC *in vivo* and *in vitro*.

Materials and methods

Cell lines and reagents. The human CRC cell lines HCT116 (TCHu 99), RKO (TCHu116), HCT15 (TCHu133) and DLD-1 (TCHu134) were purchased from and authenticated by The Cell Bank of Type Culture Collection of The Chinese Academy of Sciences. All cell lines were cultured in RPMI-1640 medium (HCT116, HCT15 and DLD-1) or DMEM (RKO) containing 10% FBS in a hypoxic cell incubator containing 1% O_2 (21%O_2 was used for normoxia)Culture medium and FBS were purchased from Gibco; Thermo Fisher Scientific, Inc. The AKT overexpression plasmid was purchased from Addgene, Inc.

Cell viability and apoptosis assays. HCT116, RKO, HCT15 and DDR-1 cells ($5x10^3$) were inoculated into 96-well plates and, after 48 h, α-hederin (Chengdu Must Bio-Technology Co., Ltd), OXA (Chia Tai Tianqing Pharmaceutical Group Co., Ltd.) or 5-FU (Chia Tai Tianqing Pharmaceutical Group Co., Ltd.) were added. After 48 h of treatment at 37˚C, cell viability was evaluated using the Cell Counting Kit 8 (CCK-8) assay (Dojindo Molecular Technologies, Inc.), and OD was detected after incubation with CCK-8 reagent for 2 h (37˚C). The IC_{50} values of different drugs were mainly determined by setting a drug concentration gradient. OD values were determined 48 h after treatment according to the previously described method and IC_{50} values were obtained according to cell survival rate. Apoptosis analysis was performed using an apoptosis detection kit (cat. no. 556547; BD Biosciences) according to the manufacturer's instructions. Apoptosis was detected using a flow cytometer (FACSCalibur; BD Biosciences), and the results were analysed by FlowJo software (V10.8.1; FlowJo, LLC).

BrdU assay. The proliferation of CRC cells (HCT116, RKO, DLD1 and HCT15) was evaluated using the cell proliferation ELISA BrdU kit (cat. no. 11647229001; Roche Diagnostics GmbH) following treatment with different concentrations of α-hederin (0, 2.5, 5, 10 and 20 μM), according to the manufacturer's instructions. The data were analysed using an ELISA reader at a wavelength of 450 nm.

JC-1 immunofluorescence assay. CRC cells ($1x10^6$) were inoculated in a six-well cell culture plate, cultured for 24 h, followed by treatment with different concentrations of α-hederin (0, 5, 10 and 20 μM) for 48 h at 37˚C. Different groups of cells were harvested and washed in PBS, and JC-1 (MedChemExpress) was added. JC-1 reagent (1 μl) was added to 500 μl 1X Incubation Buffer to provide the JC-1 working fluid, of which 500 μl was used to treat the cells. Cells were incubated with the working solution for 20 min. After washing the cells, one drop of cell suspension was added to glass slides, which were slowly covered with a cover slip, and observed under a laser confocal microscope. In the experiment, the JC-1 dye was used as a fluorescent probe, which is considered an indicator of mitochondrial membrane potential. When the mitochondrial membrane potential is high, JC-1 accumulates in the matrix of mitochondria and forms polymers, which can produce red fluorescence, whereas when the mitochondrial membrane potential is low, JC-1 cannot gather in the mitochondrial matrix, and at this time, JC-1 exists as a monomer that can produce green fluorescence. Red fluorescence indicates the presence of living cells that have maintained their mitochondrial membrane potential, whereas green fluorescence indicates the presence of cells that have undergone apoptosis or necrosis.

Reverse transcription-quantitative PCR (RT-qPCR). Total RNA was extracted from CRC cells and mouse tumour tissues using TRIzol® (Invitrogen; Thermo Fisher Scientific, Inc.), followed by RT and qPCR [95˚C for 30 sec (pre-denaturation), followed by 40 cycles at 95˚C for 5 sec (denaturation), 60˚C for 30 sec (annealing), 72˚C for 30 sec (extension)] using the PrimeScript RT-PCR kit (Takara Bio, Inc.) according to the manufacturer's instructions. The $2^{-\Delta\Delta Cq}$ method (15) was used to determine the relative expression levels in each cell line in each group. The PCR primer sequences (Accurate Biology) were as follows: Bcl2, forward 5'-TACCTGAACCGGCAC CTG-3' and reverse 5'-GCCGTACAGTTCCACAAAGG-3'; Bcl-XL, forward 5'-TTGGACAATGGACTGGTTGA-3' and reverse 5'-TGGGATGTCAGGTCACTGAA-3'; β-actin, forward 5'-ATTGCCGACAGGATGCAGAA-3' and reverse 5'-GCTGATCCACATCTGCTGGAA-3'; HIF-1α, forward 5'-ATCCATGTGACCATGAGGAATG-3' and reverse 5'-TCG GCTAGTTAGGGTACACTTC-3'.

Western blot (WB) analysis. Cells were lysed in RIPA Lysis Buffer (MedChemExpress), after which proteins were quantified using the BCA Protein Reagent Assay Kit (Beyotime Institute of Biotechnology), according to the manufacturer's instructions. Proteins (20 μg) were separated by SDS-PAGE on 10% gels and were transferred to polyvinylidene fluoride membranes. The membranes were blocked with 5% BSA (Beyotime Institute of Biotechnology) with agitation at room temperature for 1 h. Finally, the membranes were incubated with primary antibodies at 4˚C overnight and then with secondary antibodies at room temperature for 1 h. Immunoblotting was assessed using an enhanced chemiluminescent substrate (MilliporeSigma) and bands were visualized using a chemiluminescence detection system (Bio-Rad Laboratories, Inc.). The primary antibodies used were: AKT (cat. no. ab8805; 1:500), phosphorylated (p)-AKT (cat. no. ab38449; 1:1,000), STAT3 (cat. no. ab68153; 1:1,000), p-STAT3 (cat. no. ab76315; 1:5,000), cleaved Caspase-3 (cat. no. ab32042; 1:500), cleaved PARP (cat. no. ab32064; 1:2,000) (all from Abcam), HIF-1α (cat. no. 36169S; 1:1,000), Bcl2 (cat. no. 15071S; 1:1,000), Bcl-xL (cat. no. 2764S; 1:1,000) and β-actin (cat. no. 3700S; 1:1,000) (all from Cell Signaling

Technology, Inc.). Secondary antibodies (1:5,000) were also purchased from Cell Signaling Technology, Inc. (anti-mouse secondary antibody, cat. no. 7076S; anti-rabbit secondary antibody, cat. no. 7074S). Semi-quantification of protein bands was performed using ImageJ software (version 1.8.0; National Institutes of Health).

Transcriptome sequencing and analysis. Transcriptome sequencing and analysis were conducted by Shanghai OE Biotech Co., Ltd. Total cellular RNA was extracted using the TruSeq Stranded mRNA LTSample Prep Kit (cat. no. RS-122-2101; Illumina, Inc.), DNA was digested with DNase, cellular mRNA was enriched with magnetic beads containing only thymine nucleotide chains [oligo (dT)] and a breaking reagent was added to break mRNA. Using the interrupted short fragment as a template, a six-base random primer was used to synthesize one-strand cDNA, then a two-strand synthesis reaction system was prepared to synthesize two-strand cDNA, and the double-strand cDNA was purified. The purified double-strand cDNA was then subjected to end repair, an A tail was added and sequencing adapters were connected. Subsequently, fragment size selection and PCR amplification were performed. After the quality of the constructed library was assessed using an Agilent 2100 bioanalyzer (Agilent Technologies, Inc.), it was sequenced using the Illumina HiSeq™ 2500 sequencer (Illumina, Inc.) to generate 125 or 150 bp paired-end data. HiSeq X HD Reagent kit (300 cycles; cat. no. FC-501-1001; Illumina, Inc.) was used for sequencing. Library quality was assessed using the Agilent 2100 Bioanalyzer (Agilent Technologies, Inc.), and the loading concentration of the final library was >0.5 ng/G for DNA sequencing.

Subsequently, related data analysis, such as transcript level quantification, differential gene screening, functional enrichment and cluster analysis, was performed. Clean reads were sequenced with the designated reference genomes using hisat2 [(2.2.1.0) (16)] to obtain location information on reference genomes or genes, as well as specific sequence characteristics of sequenced samples. The known reference gene sequences and annotation files were used to identify the expression abundance of each protein-coding gene in each sample by sequence similarity comparison. htseq-count software [(0.9.1) (17)] was used to obtain the number of reads aligned to protein-coding genes in each sample, and cufflinks software [(2.2.1) (18)] was used to calculate the FPKM value of protein-coding gene expression. Differential expression analysis aims to identify differentially expressed genes among different samples. After obtaining differentially expressed genes, Gene Ontology (GO) functional significance and Kyoto Encyclopedia of Genes and Genomes (KEGG) pathway significance analyses were conducted.

ELISA. Cytochrome *c* and Caspase-3 levels were measured using a Cytochrome *c* ELISA kit (cat. no. ab221832; Abcam) and a Caspase-3 ELISA kit (cat. no. EK1425; Wuhan Boster Biological Technology, Ltd.), respectively. The cell supernatant was collected from each group according to the manufacturer's protocol, and a microplate reader was used to measure the optical density value at 450 nm and to calculate the experimental results.

Patient-derived tumor xenograft (PDX) models. A total of 10 patients with colorectal cancer (age, 55-65 years; six male patients, four female patients) were recruited between April 2020 and April 2021. Tissue (primary tumour tissues from patients with CRC) was collected in RPMI-1640 supplemented with penicillin and streptomycin. The mice were anesthetized with pentobarbital sodium (50 mg/kg, i.p.) before the tumour tissue was transplanted. Next, 2-3 mm^3 blocks were immediately subcutaneously transplanted on the backs of 15 male athymic nude mice (age, 5-6 weeks; weight, 20 g,; Shanghai SLAC Laboratory Animal Co., Ltd.). The mice were housed at a constant temperature of 22˚C, with a relative humidity of 30% under a 12-h light/dark cycle, and were given free access to food and water. Tumours from the first generation of mice were harvested after reaching ~1.5 cm in diameter and were directly reimplanted into a new generation of nude mice for up to five generations. The mice (n=10) were then randomly divided into the following groups: Vehicle group and α-hederin (5 mg/kg) group (n=5 mice/group); the drugs were administered by intraperitoneal injection 5 days/week for 3 weeks. Remnant tumour samples (suspended in 10% DMSO plus 10% FBS-containing RPMI-1640) were cryopreserved in liquid nitrogen for further research on other related subjects. Euthanasia was performed by intraperitoneal injection of 200 mg/kg pentobarbital. The institutional animal care and use committee of Putuo Hospital, Shanghai University of Traditional Chinese Medicine (Shanghai, China) approved all animal experiments according to the guidelines and protocols (approval no. AP202204011).

In vivo mouse model. The institutional animal care and use committee of Putuo Hospital, Shanghai University of Traditional Chinese Medicine approved all animal experiments according to the guidelines and protocols (approval no. AP202204011). A xenograft model of CRC was established via subcutaneous inoculation of 20 male athymic nude mice (age, 5-6 weeks; weight, 18-22 g; Shanghai SLAC Laboratory Animal Co., Ltd.) with $1x10^6$ normoxic and hypoxic HCT116 CRC cells. The mice were housed at a constant temperature of 22˚C, with a relative humidity of 30% under a 12-h light/dark cycle, and were given free access to food and water. After 2 weeks, the mice were divided into the following groups: Hypoxia group, normoxia group, hypoxia [α-hederin (5 mg/kg)] group and normoxia [α-hederin (5 mg/kg)] group. The drugs were administered by intraperitoneal injection 5 days/week for 4 weeks. Tumour volumes and mouse weight were measured every 4 days until the mice were euthanized by intraperitoneal injection of 200 mg/kg pentobarbital. Death was verified by the absence of heartbeat and respiration. Tumour volume (V) was calculated as follows: $V=W^2 \times L \times 0.5$, where W is the largest tumour diameter in centimetres and L is the second largest tumour diameter. Tumours were weighed after excision and fixed in 10% formalin at 4˚C for 1 week for immunohistochemistry (IHC) and haematoxylin and eosin (H&E) staining. The present study was carried out according to the National Institutes of Health Guide for the Care and Use of Laboratory Animals (19).

H&E staining. The paraffin-embedded tissue sections (5 μm) were first incubated in an automatic chip baking machine at 63˚V for 30 min. Subsequently, the sections were dehydrated,

incubated with haematoxylin (5 g/l) dyeing solution for 5 min at room temperature, washed with water, soaked in 1% hydrochloric ethanol for 3 sec, and then washed with water for a further 30 sec. After rinsing, the sections were incubated with 0.5% eosin dyeing solution for 3 min at room temperature. The sections were sealed with neutral gum and were observed under an optical microscope.

IHC. Mouse tumour tissues and tumour tissues from patients with CRC were fixed in 10% formalin at 4˚C for 1 week, embedded in paraffin and sectioned (5 μm). The paraffin-embedded tissue sections were incubated in an automatic sheet baking machine at 63˚C for 30 min, and then placed in an automatic dewaxing machine for dewaxing. The sections were then incubated with sodium citrate at high heat for 10 min and medium heat for 5 min for antigen retrieval. Subsequently, 3% H_2O_2 solution (50 μl) was added and sections were incubated in the dark at room temperature for 10 min. Then, 5% BSA sealing solution was added to the sections at 37˚C for 30 min and excess water traces were dried. Diluted primary antibodies were added (50 μl) and incubated at 4˚C overnight, followed by incubation with the diluted secondary antibody (50 μl) at 37˚C for 30 min. Subsequently, 50 μl SABC amplifiers (Wuhan Boster Biological Technology, Ltd.) were added and incubated at 37˚C for 30 min, and DAB was added for colour development. After 15 sec staining with haematoxylin, the staining was terminated and the sections were washed with water. Finally, they were dehydrated in a gradient alcohol series in a dehydrator and sealed with neutral gum. Finally, staining was observed under a microscope and images were captured. Notably, between steps, sections were washed three times with PBS (5 min/wash). IHC was performed to assess the protein expression levels of p-AKT (cat. no. 4060S; 1:200; Cell Signaling Technology, Inc.), Ki67 (cat. no. ab15580; 1:300; Abcam), Bcl2 (cat. no. ab182858; 1:500; Abcam), Bcl-xL (cat. no. ab178844; 1:1,000; Abcam) and HIF-1α (cat. no. ab114977; 1:300; Abcam). Positive staining was assessed from 10 random images of the experimental group under an optical microscope (Leica Microsystems, Inc.). The immunohistochemical staining results were assigned a mean score, considering both the intensity of staining and the proportion of tumour cells with an unequivocal positive reaction; because each section was independently evaluated by two pathologists, the score was the average of the scores of the two specialists. Each section was independently assessed by two pathologists without prior knowledge of the data. Positive reactions were defined as those showing brown signals in the cell cytoplasm. For HIF-1α, Bcl2 and Bcl- a staining index (values, 0-12) was determined by multiplying the score for staining intensity with the score for positive area. The intensity was scored as follows: 0, negative; 1, weak; 2, moderate; and 3, strong. The frequency of positive cells was defined as follows: 0, <5%; 1, 5-25%; 2, 26-50%; 3, 51-75%; and 4, >75%. When the staining was heterogeneous, it was scored as follows: Each component was scored independently and summed for the results. For example, a specimen containing 75% tumour cells with moderate intensity (3x2=6) and another 25% tumour cells with weak intensity (1x1=1) received a final score of 6+1=7. For statistical analysis, scores of 0-7 were considered low expression and scores of 8-12 were considered high expression.

Toxicity analysis. The tissues obtained from the xenograft model (heart, liver, lung, spleen, kidney and intestine) were analysed by H&E staining. Venous blood samples were collected from the eyeball after euthanasia and were placed in EDTA-coated tubes for later use in haematological studies. The samples were analysed for white blood cells, red blood cells, alanine aminotransferase, aspartate transaminase and other related indicators in the hospital clinical laboratory. Whole blood samples were centrifuged at 1,000 x g for 10 min at room temperature to obtain serum. The serum was sent to the clinical laboratory of the hospital for analysis at room temperature within 2 h of collection. The sample size for blood biochemical examination was >100 μl; the sample size for blood routine examination was >150 μl.

Colony formation assay. A total of $1x10^3$ cells were seeded in a 6-well plate, thoroughly resuspended, and cultured for 7 days in medium containing 10% FBS. Clusters containing ≥30 cells were counted as single colonies.

Cell transfection. HCT116 and RKO cells were digested and cell suspensions were spread evenly in a 6-well plate in a cell incubator. After reaching 70-90% confluence, plasmid transfection was performed. Briefly, 125 μl Opti-MEM (Invitrogen; Thermo Fisher Scientific, Inc.) and 7.5 μl Lipofectamine® 3000 reagent (Invitrogen; Thermo Fisher Scientific, Inc.) were added to an Eppendorf tube and mixed well in a biological safety cabinet. At first, 2.5 μg plasmid (plasmid backbone, pENTER) was gently mixed with 5 μl Lipofectamine 3000 and incubated for 5 min at room temperature. Subsequently, it was mixed with 125 μl Opti-MEM and incubated for 5 min at room temperature. Finally, it was mixed with 1 ml pure medium to prepare the transfection reagent. Subsequently, the prepared transfection reagent was added to the wells and shaken gently. Empty plasmids were used as negative controls. The cells were returned to the cell culture incubator, and 48 h after transfection, AKT expression levels were observed using RT-qPCR and WB analysis.

TUNEL assay. The frozen mouse tumour tissue sections stored at -80˚C were fixed with 4% paraformaldehyde for 30 min at room temperature. After fixation, sections were washed with PBS twice (10 min/wash), and 0.1% Triton X-100 was prepared with PBS and used to permeabilize tissues at room temperature for 20 min. Subsequently, sections were again washed twice with (10 min/wash) and TUNEL test solution was added to the tissue for 60 min at room temperature in the dark. After staining, sections were washed once with PBS for 5 min, sealed with anti-fluorescence quenching sealing liquid and observed under a laser confocal microscope. The excitation wavelength was 488 nm and the emission wavelength range was 515-565 nm.

Statistical analysis. All data are reported as the mean ± SD from triplicate experiments and were analysed using SPSS 22.0 (IBM Corporation). Unpaired Student's t-test or Mann-Whitney U test was performed for comparisons between two groups, and Tukey's post-hoc test was performed for pairwise comparisons among multiple groups following one-way ANOVA or two-way ANOVA. The correlation coefficients were analysed

using the Spearman's rank test. P<0.05 was considered to indicate a statistically significant difference.

Results

α-hederin overcomes hypoxia-mediated drug resistance in CRC cells. It has previously been reported that hypoxia promotes chemoresistance. In the present study, it was revealed that hypoxia caused CRC cell resistance to OXA and 5-FU, whereas hypoxia did not cause CRC cell resistance to α-hederin (Fig. S1A and B). The results of the CCK-8 assay revealed that under normoxic and hypoxic conditions, α-hederin inhibited the viability of CRC cells, suggesting that α-hederin may overcome hypoxia-mediated resistance in CRC cells (Fig. 1A). The cell colony formation and BrdU assay results demonstrated that α-hederin effectively inhibited CRC cell colony formation under normoxia and hypoxia (Fig. 1B and C). Taken together, these results suggested that α-hederin may inhibit the viability and proliferation of CRC cells under hypoxia and that its inhibitory effect is similar to that under normoxia.

Apoptotic pathway serves a key role in the effects of α-hederin in overcoming hypoxia-mediated resistance in CRC cells. The *in vitro* molecular mechanism by which α-hederin overcomes hypoxia-mediated resistance in CRC cells was subsequently assessed. The follow-up experiments were performed in a representative sample of colorectal cancer cells (HCT116 and RKO). Transcriptome sequencing analysis revealed that apoptosis-related pathways were downregulated in HCT116 cells under hypoxia (Fig. S2A-C), and high expression levels of Bcl2 (Fig. S3A-C) and Bcl-xL (Fig. S3B and C) was found in CRC cells under hypoxia, suggesting that they may be key factors in the process of hypoxia-mediated resistance. Firstly, the differentially expressed genes (including upregulated and downregulated genes) between the hypoxia group and the drug treatment group were visualized using a volcano plot (Fig. 2A), and GO and KEGG functional enrichment analyses were subsequently performed (Fig. 2B and C). The results revealed that the effect of α-hederin on CRC under hypoxia was mainly related to the apoptosis pathway. In addition, gene expression profiling showed that the Bcl2 transcription level changed most obviously after α-hederin treatment of CRC cells under hypoxia (Fig. 2D), suggesting that α-hederin may reduce the expression of the antiapoptotic gene Bcl2 to overcome the resistance of CRC cells to hypoxia. RT-qPCR analysis further confirmed that the expression levels of Bcl2 and Bcl-xL were decreased following treatment of CRC cells with α-hederin under hypoxia for 48 h (Fig. 2E). In summary, these data indicated that the apoptotic pathway may serve a key role in the mechanism by which α-hederin inhibits the proliferation of CRC cells under hypoxic conditions.

α-hederin overcomes drug resistance in CRC cells under hypoxic conditions by promoting apoptosis. To confirm that α-hederin can overcome hypoxia-mediated resistance in CRC by promoting apoptosis, apoptosis assays were performed. Annexin V/propidium iodide staining revealed that the apoptotic rate (early + late) of hypoxic CRC cells was significantly increased following treatment with α-hederin for 48 h in a dose-dependent manner (Fig. 3A). In addition, the JC-1 immunofluorescence assay demonstrated that with increasing drug concentration, the intensity of green fluorescence changed from weak to strong, indicating that apoptosis gradually increased (Fig. 3B). Moreover, the activities of apoptosis-related indicators, such as cytochrome *c* and Caspase-3, were significantly increased in a dose-dependent manner, as determined by ELISA (Fig. 3C). After α-hederin treatment of CRC cells under hypoxic conditions, the expression levels of Bcl2 and Bcl-xL were decreased, whereas the expression levels of Bax, cleaved Caspase-3 and cleaved PARP were increased (Fig. 3D). Taken together, these results suggested that α-hederin may inhibit the proliferation of CRC cells under hypoxic conditions by promoting apoptosis.

AKT/Bcl2 signalling pathway is a key mechanism by which α-hederin overcomes hypoxia-mediated resistance in CRC cells. The present study also assessed whether Bcl-2 serves a key role in the effects of α-hederin on overcoming hypoxia-mediated resistance. A previous study indicated that HIF-1α can affect Bcl2 expression (20). The results of WB and RT-qPCR analyses revealed that there was no change in the expression levels of HIF-1α in CRC cells treated with α-hederin under hypoxic conditions, suggesting that α-hederin does not overcome hypoxia-mediated resistance by inhibiting the expression of HIF-1α (Fig. 4A and B). Sequencing analysis results suggested that the AKT signalling pathway was altered under hypoxia (Fig. S2C), and the levels of p-AKT and p-STAT3 were increased in CRC cells under hypoxia (Fig. S3C). However, the results of WB analysis showed that p-AKT levels were decreased in whole-cell lysates following α-hederin treatment, whereas p-STAT3 levels were not affected (Figs. 4A, S4A and B). In addition, RT-qPCR demonstrated that the mRNA expression levels of Bcl2 and Bcl-xL were decreased (Fig. 4B). The successful overexpression of AKT in CRC cells was verified by RT-qPCR and WB analyses (Fig. S4C and D). Notably, when AKT expression was rescued in CRC cells, the inhibitory effect of α-hederin on Bcl2 and Bcl-xL expression was mitigated (Fig. 4C and D). In addition, the role of AKT in the regulatory effects of α-hederin on CRC cell apoptosis under hypoxic conditions was further explored. The results revealed that the proapoptotic effect of α-hederin was weakened in CRC cells overexpressing AKT (Fig. 4E-H); the apoptotic rate and the levels of apoptosis-related indicators (cytochrome *c* and Caspase-3) were decreased. These results indicated that the AKT/Bcl2 signalling pathway may be the key mechanism by which α-hederin inhibits CRC cell proliferation under hypoxic conditions.

α-hederin overcomes hypoxia-mediated resistance in CRC via the AKT/Bcl2 pathway in vivo. To further explore the role of α-hederin in overcoming hypoxia-mediated resistance in CRC *in vivo*, a xenograft mouse model with HCT116 cells was established. The results revealed that α-hederin inhibited tumour growth in both the hypoxia and normoxia groups (Fig. 5A and C). In addition, α-hederin reduced the expression levels of Bcl2 and Bcl-xL in the tissues of mice in the hypoxia group (Fig. 5D). Consistent with the results of the previous cell experiments, the expression levels of HIF-1α in the hypoxia group did not alter after α-hederin treatment, whereas the levels of Ki67 (an indicator of cell proliferation),

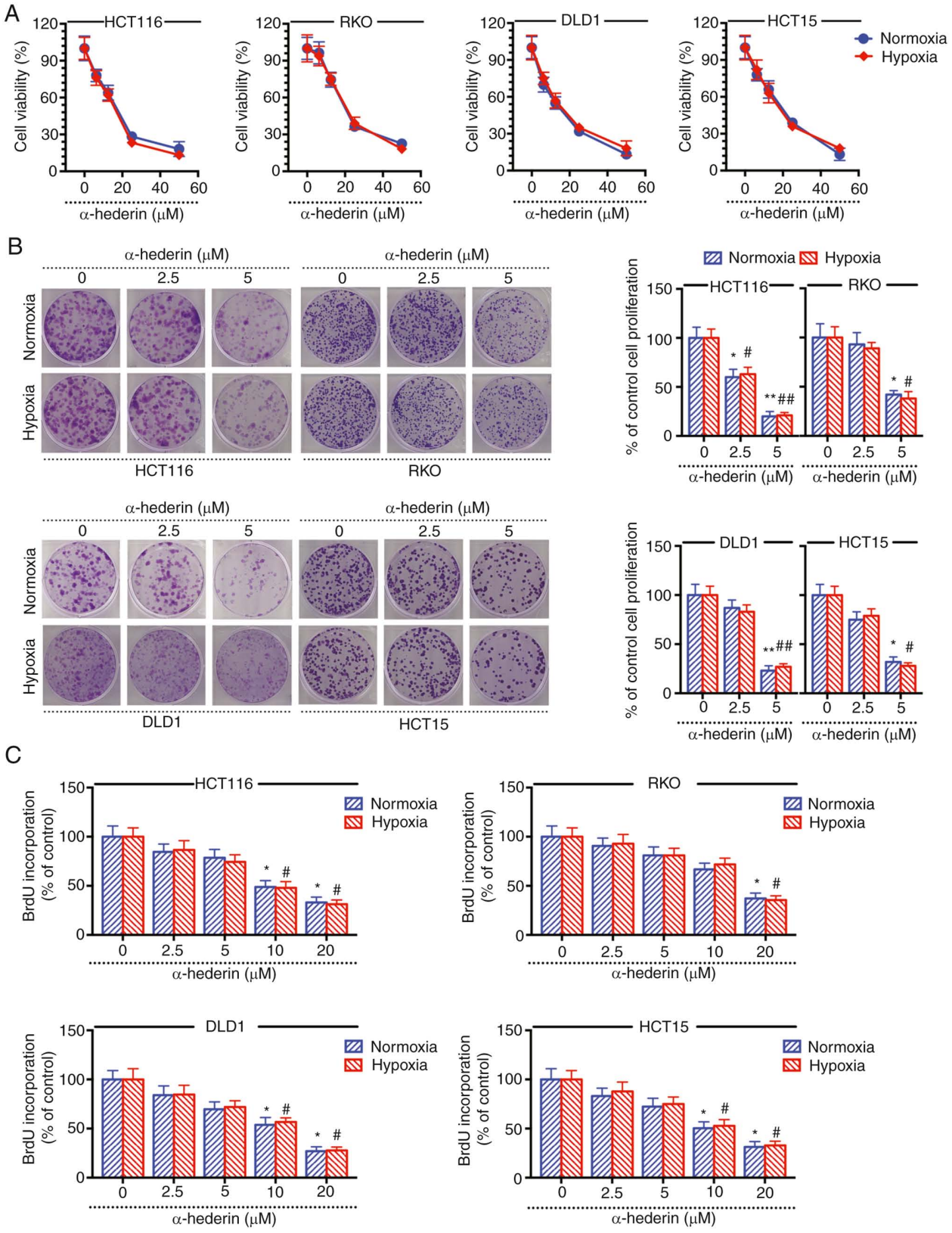

Figure 1. α-hederin overcomes hypoxia-mediated drug resistance in colorectal cancer cells. (A) Effect of α-hederin on the viability of different types of cells under normoxia and hypoxia. (B) Colony formation assay showed the effect of α-hederin on the proliferation of different types of cells under normoxia and hypoxia. (C) BrdU experiment showed the effect of α-hederin on the proliferation of different types of cells under normoxia and hypoxia. Data are presented as the mean ± SD. Compared to control group treated with no drugs, $^{*,\#}P<0.05$, $^{**,\#\#}P<0.01$ vs. control group (0 μM).

Bcl2, Bcl-xL, and p-AKT were decreased, as shown by IHC (Fig. 5B). In addition, the TUNEL assay results showed that the green fluorescence intensity was enhanced in response to α-hederin treatment, thus indicating increased apoptosis (Fig. 5B). Furthermore, the body weight of mice in different groups was not significantly affected, indicating that the drug

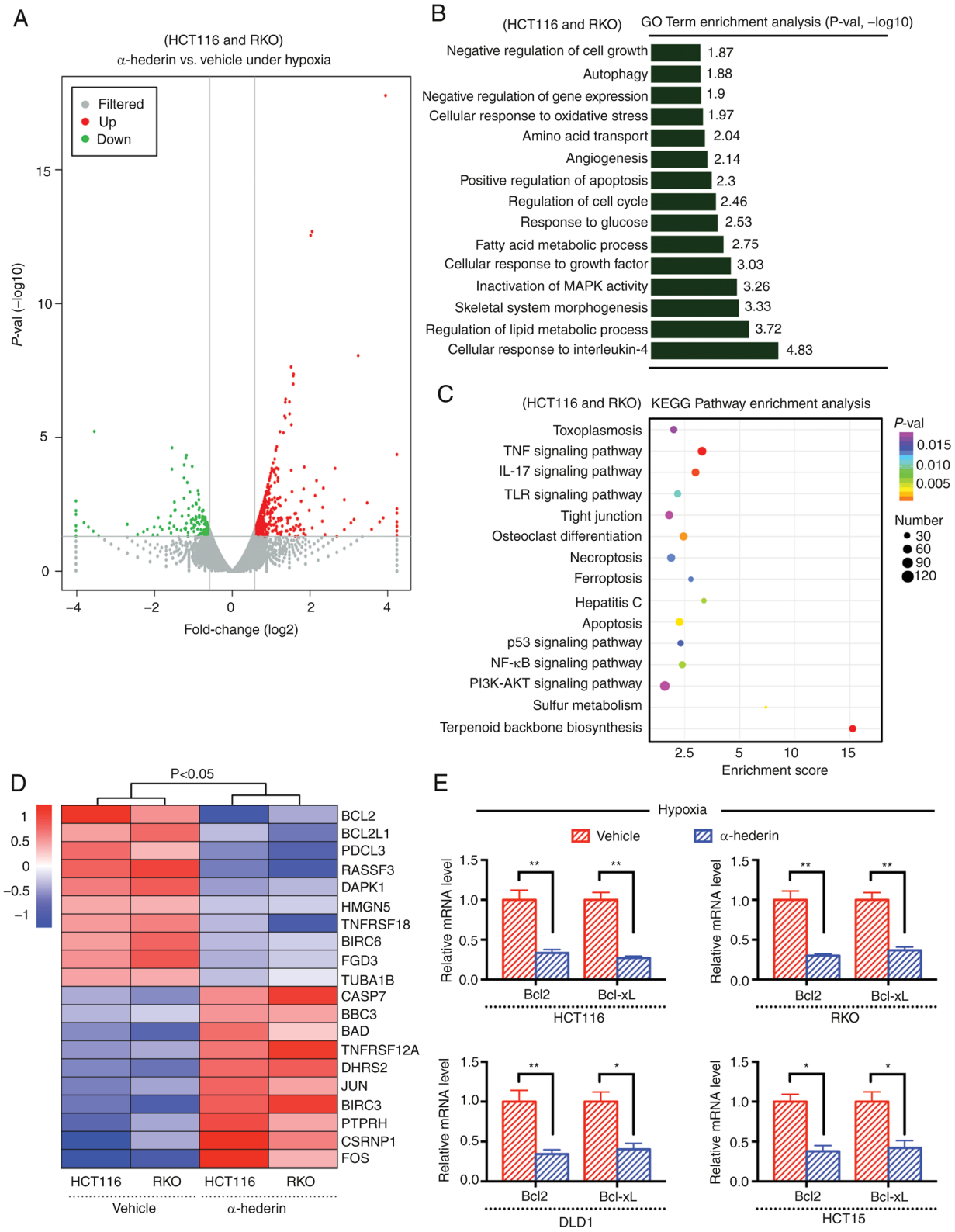

Figure 2. Apoptotic pathway serves a key role in the effects of α-hederin on overcoming hypoxia-mediated resistance in CRC cells. (A) Differentially expressed genes were observed in a volcano plot. (B) Enrichment analysis of GO terms. (C) Enrichment analysis of KEGG pathways. (D) Gene expression profiling was conducted to observe the changes in related genes after α-hederin treatment of CRC cells under hypoxia. (E) Reverse transcription-quantitative PCR was used to measure the expression levels of Bcl2 and Bcl-xL in CRC cells treated with α-hederin under hypoxia. Data are presented as the mean ± SD. *P<0.05, **P<0.01. CRC, colorectal cancer; GO, Gene Ontology; KEGG, Kyoto Encyclopedia of Genes and Genomes.

treatments exerted no obvious toxicity (Fig. 5E). There was no significant change in the biochemical indicators of the orbital blood collected from the nude mice in each group (Fig. 5F). H&E staining confirmed that the organs were intact, without damage, and nuclei were clearly visible, suggesting that α-hederin had no obvious toxicity *in vivo* (Fig. 5G). In

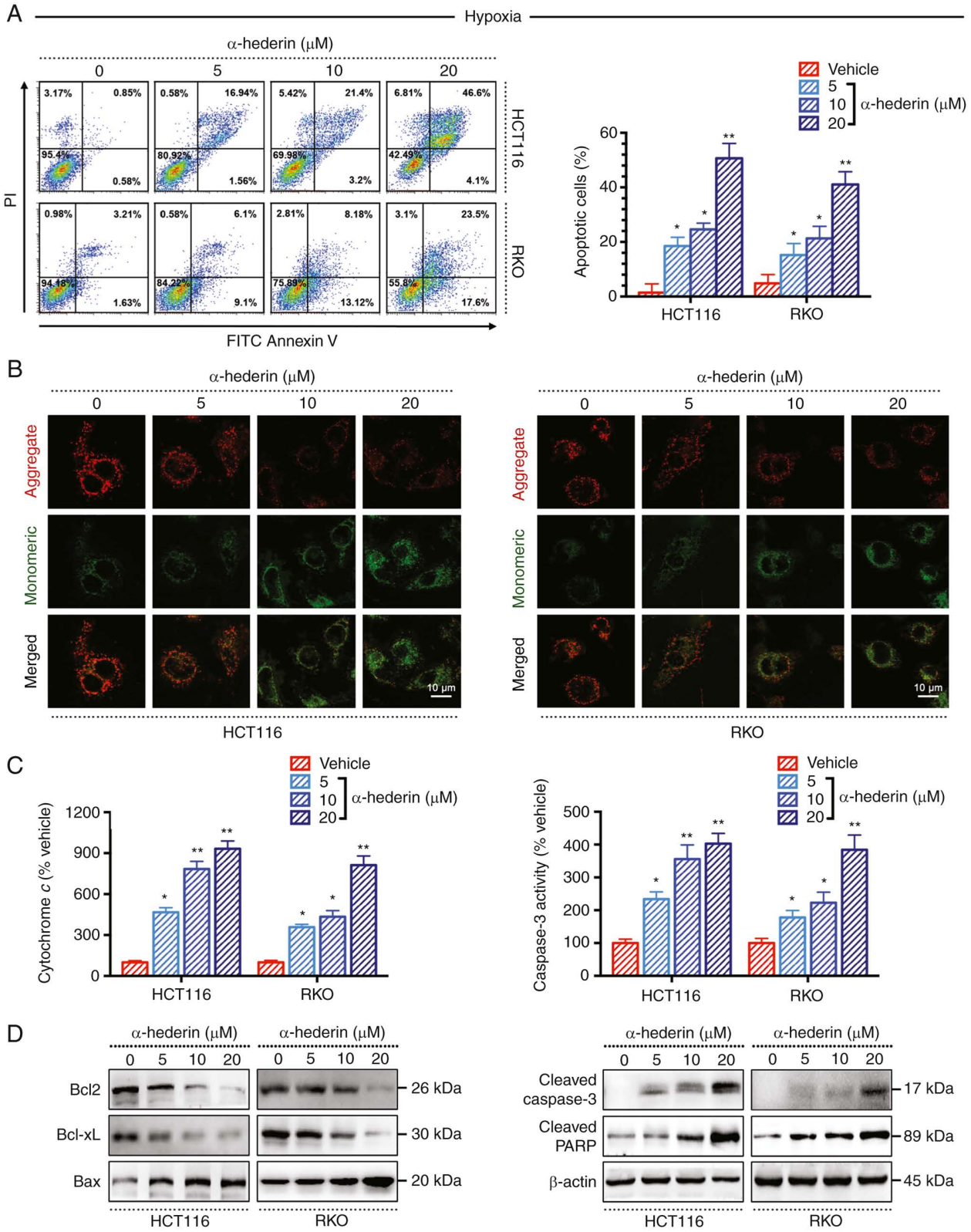

Figure 3. α-hederin overcomes drug resistance in CRC cells under hypoxic conditions by promoting apoptosis. (A) Flow cytometry and (B) JC-1 immunofluorescence assays were used to evaluate the apoptosis of hypoxic CRC cells treated with α-hederin. (C) ELISA was used to observe the activities of cytochrome *c* and Caspase-3 after α-hederin treatment. (D) Western blot analysis was used to measure the expression levels of apoptosis-related proteins after α-hederin treatment of CRC cells under hypoxia; β-actin blot is the loading control blot for all of the proteins. Data are presented as the mean ± SD. *P<0.05, **P<0.01 vs. vehicle. CRC, colorectal cancer; PI, propidium iodide.

summary, these data suggested that α-hederin overcomes hypoxia-mediated resistance in CRC cells *in vivo* through the AKT/Bcl2 signalling pathway.

α-hederin overcomes hypoxia-mediated resistance by reducing Bcl2 and Bcl-xL expression in a PDX mouse model. An important association has previously been reported

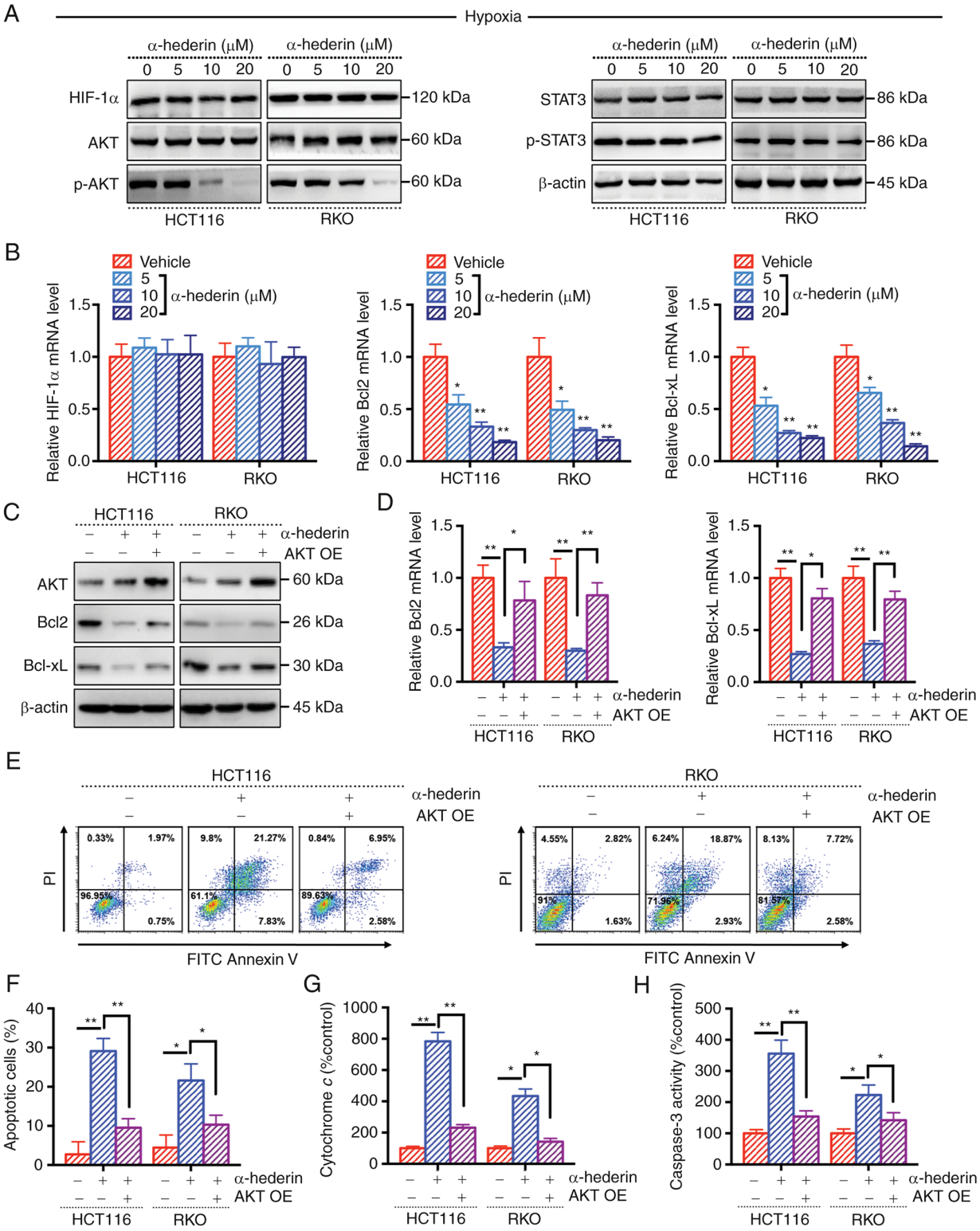

Figure 4. AKT/Bcl2 signalling pathway is a key mechanism by which α-hederin overcomes hypoxia-mediated resistance in CRC cells. (A) Treatment of hypoxic CRC cells with α-hederin affected the expression of related proteins, as determined by western blot analysis, β-actin blot is the loading control blot for all of the proteins. (B) Reverse transcription-quantitative PCR was used to measure the expression levels of HIF-1α, Bcl2 and Bcl-xL after α-hederin treatment of hypoxic CRC cells. After OE of AKT, the effect of α-hederin treatment on the (C) protein and (D) mRNA expression levels of Bcl2 and Bcl-xL in hypoxic CRC cells was observed. (E and F) After OE of AKT, the apoptosis of hypoxic CRC cells treated with α-hederin was evaluated. After OE of AKT, the levels of (G) cytochrome *c* and (H) Caspase 3 were observed after α-hederin treatment of hypoxic CRC cells. Data are presented as the mean ± SD. *P<0.05, **P<0.01 vs. vehicle or as indicated. CRC, colorectal cancer; OE, overexpression; p-, phosphorylated; PI, propidium iodide.

between HIF-1α and Bcl2 (21). Herein, the expression levels of Bcl2 and Bcl-xL were observed to be positively correlated with the expression levels of HIF-1α in the collected clinical tissue samples, as demonstrated by IHC experiments, indicating that apoptosis inhibition was positively correlated with hypoxia (Fig. 6A-C). In addition, a PDX model in mice

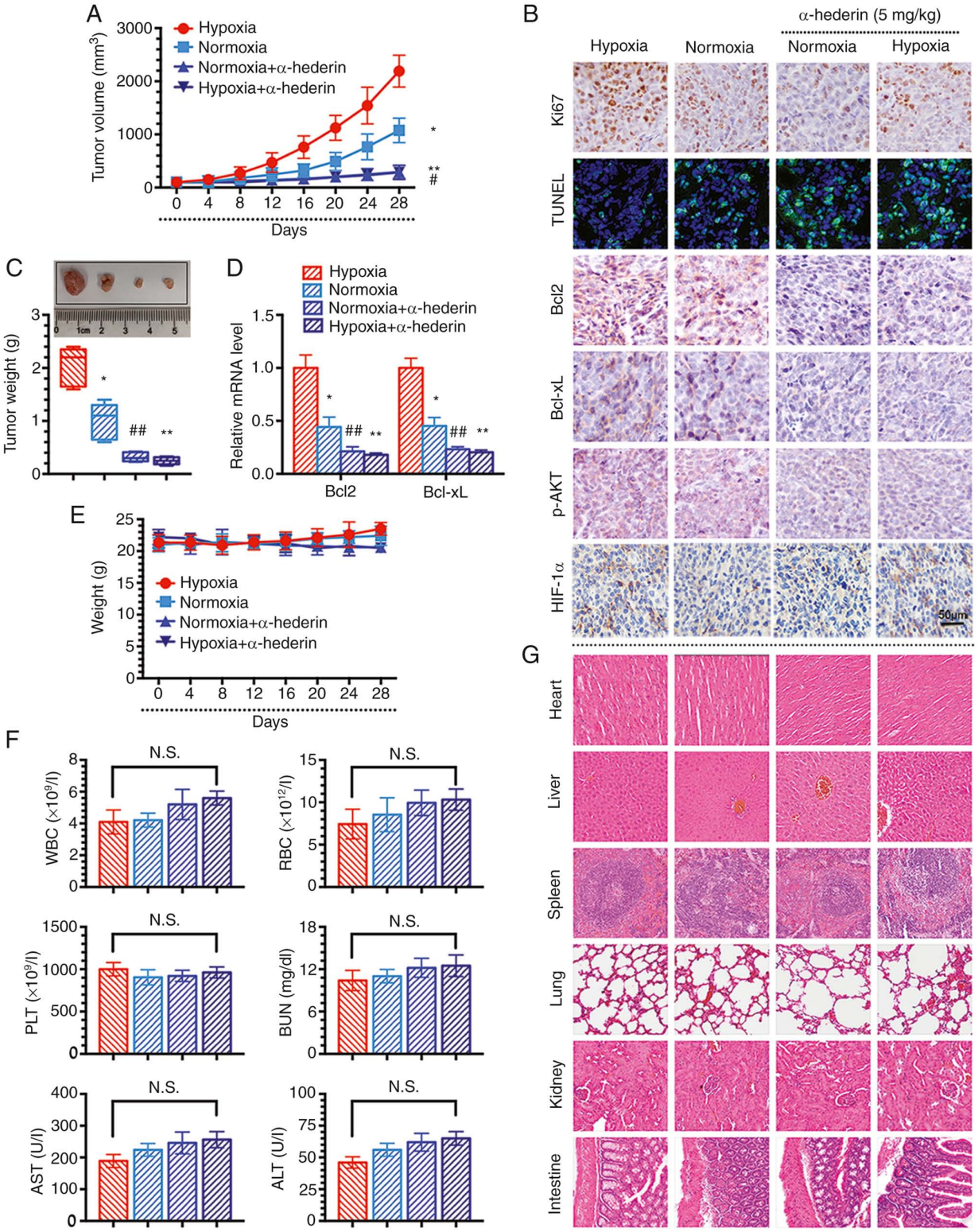

Figure 5. α-hederin overcomes hypoxia-mediated resistance in colorectal cancer cells via the AKT/Bcl2 pathway *in vivo*. (A) Xenograft tumour growth curves. (B) Representative images of the immunohistochemical staining of Ki67, Bcl2, Bcl-xL, p-AKT and HIF-1α in tissues and the evaluation of apoptosis in each group by TUNEL. Scale bars, 50 μm. (C) Images and weights of tumours. (D) Reverse transcription-quantitative PCR was used to measure the expression levels of Bcl2 and Bcl-xL in tissues. (E) Mouse weight curves after treatment in the CRC xenograft model. (F) Detection of changes in blood biochemical indicators in mice. (G) Haematoxylin and eosin staining to observe organ damage (magnification, x100). Data are presented as the mean ± SD. *P<0.05, **P<0.01 vs. hypoxia; $^{\#}$P<0.05, $^{\#\#}$P<0.01 vs. normoxia. ALT, alanine aminotransferase; AST, aspartate aminotransferase; N.S., not significant; RBC, red blood cell; PLT, platelets; WBC, white blood cell.

was further established, and it was revealed that α-hederin inhibited tumour growth (Fig. 6D-G). Furthermore, α-hederin reduced the expression levels of Bcl2 and Bcl-xL in the tissues (Fig. 6F and G). There was no significant change in the expression levels of HIF-1α following treatment with α-hederin, whereas the expression levels of Ki67, Bcl2 and

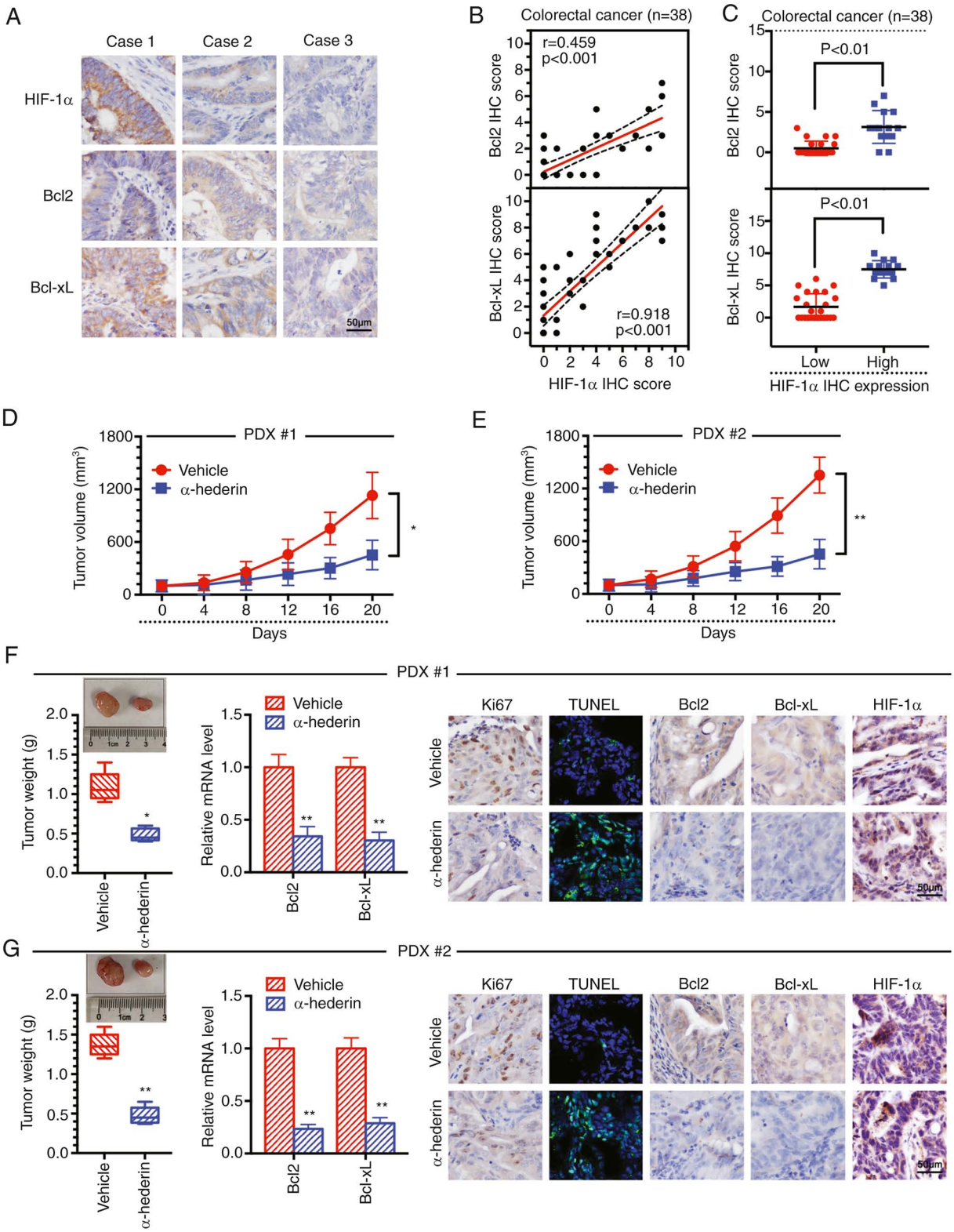

Figure 6. α-hederin overcomes hypoxia-mediated resistance by reducing Bcl2 and Bcl-xL expression in PDX mouse models. (A) Immunohistochemical analysis of HIF-1α and anti-apoptotic proteins in clinical tissue samples. (B) Immunohistochemical score was used to analyse the correlation between HIF-1α expression and anti-apoptotic protein expression. (C) The relationship between HIF-1α expression levels and immunohistochemical score of anti-apoptotic proteins is shown. (D and E) PDX growth curves in mice. (F and G) Images and weights of tumours. RT-qPCR was used to measure the expression levels of Bcl2 and Bcl-xL in tissues. Representative images of IHC of Ki67, Bcl2, Bcl-xL, p-AKT and HIF-1α in tissues and evaluation of apoptosis in each group by TUNEL. Scale bars, 50 μm. Data are presented as the mean ± SD. *P<0.05, **P<0.01 vs. vehicle or as indicated. IHC, immunohistochemistry; PDX, patient-derived xenograft.

Bcl-xL were decreased, as demonstrated by IHC experiments (Fig. 6F and G). In addition, the TUNEL assay results showed that the fluorescence intensity gradually increased, indicating that the degree of apoptosis in the tissue increased after

α-hederin treatment (Fig. 6F and G). These data suggested that α-hederin overcomes hypoxia-mediated resistance in PDX mouse models by reducing Bcl2 and Bcl-xL expression.

Discussion

The morbidity and mortality of patients with CRC currently show an increasing trend (22). To date, chemotherapy is still considered the mainstay of treatment for CRC; however, clinical studies have revealed that a number of tumours are likely to develop resistance to chemotherapy, ultimately leading to treatment failure (23). Related research has shown that the hypoxic microenvironment can promote tumour resistance (24,25). One of the main mechanisms of tumour resistance is the inhibition of apoptosis caused by overexpression of anti-apoptotic proteins. Hypoxia-induced tumour resistance via inhibition of the apoptotic signalling pathway has attracted increasing attention (26).

Bcl2 family oncoproteins serve an important role in regulating apoptosis. Specifically, abnormal Bcl2 activation is associated with the occurrence and progression of various types of cancer, and has become a key indicator for evaluating clinical efficacy and prognosis (27-30). In the hypoxic microenvironment, the expression of Bcl2 in tumours can increase, whereas the expression of proapoptotic proteins decreases. In the present study, the protein and mRNA expression levels of anti-apoptotic genes were revealed to be significantly increased under hypoxia. Notably, hypoxia activated and regulated AKT phosphorylation to increase the expression of Bcl2 and exert an anti-apoptotic effect. The sensitivity of malignant tumour cells to apoptosis has been reported to be effectively increased by either reducing Bcl2 protein levels or inhibiting Bcl2 activity (31).

A growing number of studies have elucidated the effect of traditional Chinese medicines on inhibiting hypoxia-mediated tumour development (32-34). α-hederin, also referred to as koronaroside A or sapindoside A, is a monodesmosidic triterpenoid saponin that widely exists throughout the plant kingdom, including in *Hedera* and *Nigella* species (35). Related studies have reported that α-hederin possesses biological and pharmacological properties. (36-38). α-hederin has recently attracted attention for its marked antitumour potential, as it exhibits cytotoxic activity against various cancer cell lines by inhibiting cell proliferation and promoting apoptosis *in vitro* and *in vivo* (39,40). In the present study, obvious resistance to the chemotherapeutic drugs OXA and 5-FU was observed under hypoxic conditions, and α-hederin may overcome hypoxia-induced resistance in CRC cells.

Further studies have reported that α-hederin reduces the phosphorylation of AKT and the expression of Bcl2 in CRC under hypoxic conditions, suggesting that the regulation of AKT phosphorylation can overcome hypoxia-mediated resistance in CRC cells. In addition, the levels of cytochrome *c* and Caspase-3 were decreased in a dose-dependent manner after α-hederin treatment in the present study, which also verified from another experimental perspective that α-hederin can overcome hypoxia-mediated resistance in CRC cells. Furthermore, it was demonstrated that α-hederin decreased Bcl2 expression in CRC cells by inhibiting p-AKT in rescue experiments. *In vivo*, α-hederin significantly overcame hypoxia-mediated resistance in different mouse models via the AKT/Bcl2 signalling pathway. In addition, in animal experiments it was observed that the mice treated with α-hederin did not exhibit toxic side effects. There was no marked change in the biochemical indicators of the orbital blood of nude mice. In addition, H&E staining confirmed that the organs were intact, without damage, and nuclei were clearly visible, especially in the intestinal tissue, suggesting that α-hederin had no obvious toxicity *in vivo*. Upon reviewing the literature, no related reports that indicated α-hederin affects normal colonic epithelial cells were found. In addition, the expression levels of Bcl2 and Bcl-xL were revealed to be positively correlated with the expression levels of HIF-1α in clinical tissues, thus indicating that there may be a positive correlation between hypoxia and inhibition of apoptosis.

In conclusion, the present study identified that α-hederin can overcome hypoxia-mediated resistance in CRC via the AKT/Bcl2 pathway *in vivo* and *in vitro*. The results of the present study may provide a reliable basis for the clinical comprehensive treatment of CRC, particularly treatment with adjuvant drugs that have α-hederin as the main active ingredient. In the future, α-hederin may be used as a novel adjuvant for reversing drug resistance in CRC.

Acknowledgements

Not applicable.

Funding

This project was sponsored by the Natural Science Foundation of Shanghai (grant no. 20ZR1450500), the Clinical Specialized Disease Construction Project of Shanghai Putuo District Municipal Health Commission (grant no. 2020tszb03), the Shanghai Rising-Star Program (Sailing Special Project, grant no. 22YF1441400), the Shanghai Key Medical Specialty Construction Project (grant no. ZK2019B18), the Independent Innovation Project in Putuo District (grant no. ptkwws201701), the Chengdu University of Traditional Chinese Medicine 'Xinglin Scholars' Discipline Talents Research Promotion Plan (grant no. YYZX2020120) and the budget project of Shanghai University of Traditional Chinese Medicine (grant no. 2020LK072).

Availability of data and materials

The datasets used and/or analysed during the current study are available from the corresponding author on reasonable request. Sequencing data have been deposited in NCBI Sequence Read Archive under the accession code PRJNA912906 (https://www.ncbi.nlm.nih.gov/bioproject/?term=PRJNA912906).

Authors' contributions

WL and KX conceived and designed the study. JC, JX and JY collected the data, and analysed and interpreted the data. JC and JX drafted the article. WD, LJ, WW, XS, DZ, SL, PY, YZ and YC and KY performed some of the experiments and aided in the construction of the tumour model. SL, PY, YZ and YC critically revised the article. All authors read and approved the

final manuscript. All authors confirmed the authenticity of all the raw data.

Ethics approval and consent to participate

All patient samples were obtained with oral informed consent and the approval of the ethics committee of Putuo Hospital, Shanghai University of Traditional Chinese Medicine (app roval no. PTEC-A-2021-29-1). All animal experiments were conducted in accordance with guidelines and protocols approved by the institutional animal care and use committee of Putuo Hospital, Shanghai University of Traditional Chinese Medicine (approval no. AP202204011).

Patient consent for publication

Not applicable.

Competing interests

The authors declare that they have no competing interests.

References

1. de Oliveira MB, Koshkin V, Liu G and Krylov SN: Analytical challenges in development of chemoresistance predictors for precision oncology. Anal Chem 92: 12101-12110, 2020.
2. Akman M, Belisario DC, Salaroglio IC, Kopecka J, Donadelli M, De Smaele E and Riganti C: Hypoxia, endoplasmic reticulum stress and chemoresistance: Dangerous liaisons. J Exp Clin Cancer Res 40: 28, 2021.
3. McAleese CE, Choudhury C, Butcher NJ and Minchin RF: Hypoxia-mediated drug resistance in breast cancers. Cancer Lett 502: 189-199, 2021.
4. Dzhalilova DS and Makarova OV: HIF-dependent mechanisms of relationship between hypoxia tolerance and tumor development. Biochemistry (Mosc) 86: 1163-1180, 2021.
5. Zhang M, Liu Q, Li L, Ning J, Tu J, Lei X, Mo Z and Tang S: Cytoplasmic M-CSF facilitates apoptosis resistance by inhibiting the HIF-1α/BNIP3/Bax signalling pathway in MCF-7 cells. Oncol Rep 41: 1807-1816, 2019.
6. Xu D, Li DW, Xie J and Chen XW: Effect and mechanism of survivin on hypoxia-induced multidrug resistance of human laryngeal carcinoma cells. Biomed Res Int 2019: 5696801, 2019.
7. Yun CW, Lee JH and Lee SH: Hypoxia-induced PGC-1α regulates mitochondrial function and tumorigenesis of colorectal cancer cells. Anticancer Res 39: 4865-4876, 2019.
8. Wang Y, Qi Z, Zhou M, Yang W, Hu R, Li G, Ma X and Zhang Z: Stanniocalcin-1 promotes cell proliferation, chemoresistance and metastasis in hypoxic gastric cancer cells via Bcl-2. Oncol Rep 41: 1998-2008, 2019.
9. Zeng J, Huang T, Xue M, Chen J, Feng L, Du R and Feng Y: Current knowledge and development of hederagenin as a promising medicinal agent: A comprehensive review. RSC Adv 8: 24188-24202, 2018.
10. Wang J, Wu D, Zhang J, Liu H, Wu J and Dong W: α-Hederin induces apoptosis of esophageal squamous cell carcinoma via an oxidative and mitochondrial-dependent pathway. Dig Dis Sci 64: 3528-3538, 2019.
11. Liu Y, Lei H, Ma J, Deng H, He P and Dong W: α-Hederin increases the apoptosis of cisplatin-resistant gastric cancer cells by activating mitochondrial pathway in vivo and vitro. Onco Targets Ther 12: 8737-8750, 2019.
12. Sun J, Feng Y, Wang Y, Ji Q, Cai G, Shi L, Wang Y, Huang Y, Zhang J and Li Q: α-hederin induces autophagic cell death in colorectal cancer cells through reactive oxygen species dependent AMPK/mTOR signaling pathway activation. Int J Oncol 54: 1601-1612, 2019.
13. Fang C, Liu Y, Chen L, Luo Y, Cui Y, Zhang N, Liu P, Zhou M and Xie Y: α-Hederin inhibits the growth of lung cancer A549 cells in vitro and in vivo by decreasing SIRT6 dependent glycolysis. Pharm Biol 59: 11-20, 2021.
14. Wang J, Deng H, Zhang J, Wu D, Li J, Ma J and Dong W: α-Hederin induces the apoptosis of gastric cancer cells accompanied by glutathione decrement and reactive oxygen species generation via activating mitochondrial dependent pathway. Phytother Res 34: 601-611, 2020.
15. Livak KJ and Schmittgen TD: Analysis of relative gene expression data using real-time quantitative PCR and the 2(-Delta Delta C(T)) method. Methods 25: 402-408, 2001.
16. Kim D, Langmead B and Salzberg SL: HISAT: A fast spliced aligner with low memory requirements. Nat Methods 12: 357-360, 2015.
17. Anders S, Pyl PT and Huber W: HTSeq-a Python framework to work with high-throughput sequencing data. Bioinformatics 31: 166-169, 2015.
18. Roberts A, Pimentel H, Trapnell C and Pachter L: Identification of novel transcripts in annotated genomes using RNA-Seq. Bioinformatics 27: 2325-2329, 2011.
19. Zhan Y, Qiu Y, Wang H, Wang Z, Xu J, Fan G, Xu J, Li W, Cao Y, Le VM, *et al*: Bufalin reverses multidrug resistance by regulating stemness through the CD133/nuclear factor-κB/MDR1 pathway in colorectal cancer. Cancer Sci 111: 1619-1630, 2020.
20. Zhao X, Liu L, Li R, Wei X, Luan W, Liu P and Zhao J: Hypoxia-inducible factor 1-α (HIF-1α) induces apoptosis of human uterosacral ligament fibroblasts through the death receptor and mitochondrial pathways. Med Sci Monit 24: 8722-8733, 2018.
21. Valladares KJP, Balbinot KM, de Moraes AT, Kataoka MSDS, Ramos AMPC, Ramos RTJ, da Silva ALDC, Mesquita RA, Normando D, Júnior SM and de Jesus Viana Pinheiro J: HIF-1α is associated with resistance to hypoxia-induced apoptosis in ameloblastoma. Int J Dent 2021: 3060375, 2021.
22. Ding Q, Kong X, Zhong W and Liu W: Fecal biomarkers: Non-invasive diagnosis of colorectal cancer. Front Oncol 12: 971930, 2022.
23. Zhang L, Lu Z and Zhao X: Targeting Bcl-2 for cancer therapy. Biochim Biophys Acta Rev Cancer 1876: 188569, 2021.
24. Belisario DC, Kopecka J, Pasino M, Akman M, De Smaele E, Donadelli M and Riganti C: Hypoxia dictates metabolic rewiring of tumors: Implications for Chemoresistance. Cells 9: 2598, 2020.
25. Liu J, Gao L, Zhan N, Xu P, Yang J, Yuan F, Xu Y, Cai Q, Geng R and Chen Q: Hypoxia induced ferritin light chain (FTL) promoted epithelia mesenchymal transition and chemoresistance of glioma. J Exp Clin Cancer Res 39: 137, 2020.
26. Cao Y, Jiang Z, Zeng Z, Liu Y, Gu Y, Ji Y, Zhao Y and Li Y: Bcl-2 silencing attenuates hypoxia-induced apoptosis resistance in pulmonary microvascular endothelial cells. Apoptosis 21: 69-84, 2016.
27. Letai A, Sorcinelli MD, Beard C and Korsmeyer SJ: Antiapoptotic BCL-2 is required for maintenance of a model leukemia. Cancer Cell 6: 241-249, 2004.
28. Goff DJ, Recart AC, Sadarangani A, Chun HJ, Barrett CL, Krajewska M, Leu H, Low-Marchelli J, Ma W, Shih AY, *et al*: A Pan-BCL2 inhibitor renders bone-marrow-resident human leukemia stem cells sensitive to tyrosine kinase inhibition. Cell Stem Cell 12: 316-328, 2013.
29. Delbridge AR, Grabow S, Strasser A and Vaux DL: Thirty years of BCL-2: Translating cell death discoveries into novel cancer therapies. Nat Rev Cancer 16: 99-109, 2016.
30. Lee J, Sohn EJ, Yoon SW, Kim CG, Lee S, Kim JY, Baek N and Kim SH: Anti-metastatic effect of dehydrocorydaline on H1299 non-small cell lung carcinoma cells via inhibition of matrix metalloproteinases and B cell lymphoma 2. Phytother Res 31: 441-448, 2017.
31. Davids MS and Letai A: ABT-199: Taking dead aim at BCL-2. Cancer Cell 23: 139-141, 2013.
32. Li JR, Ren J, Yang SC, Han JQ, Guo YJ and Ji ES: Effect of xiaotan huayu liqiao traditional Chinese medicine compound on myocardial fibrosis in rats with chronic intermittent hypoxia and its mechanism. Zhongguo Ying Yong Sheng Li Xue Za Zhi 36: 414-418, 2020 (In Chinese).
33. Peng W, Zhang S, Zhang Z, Xu P, Mao D, Huang S, Chen B, Zhang C and Zhang S: Jianpi Jiedu decoction, a traditional Chinese medicine formula, inhibits tumorigenesis, metastasis, and angiogenesis through the mTOR/HIF-1α/VEGF pathway. J Ethnopharmacol 224: 140-148, 2018.
34. Li RL, He LY, Zhang Q, Liu J, Lu F, Duan HX, Fan LH, Peng W, Huang YL and Wu CJ: HIF-1α is a potential molecular target for herbal medicine to treat diseases. Drug Des Devel Ther 14: 4915-4949, 2020.

35. Rooney S and Ryan MF: Efects of α-hederin and thymoquinone, constituents of Nigella sativa, on human cancer cell lines. Anticancer Res 25: 2199-2204, 2005.
36. Lorent JH, Léonard C, Abouzi M, Akabi F, Quetin-Leclercq J and Mingeot-Leclercq MP: α-Hederin induces apoptosis, membrane permeabilization and morphologic changes in two cancer cell lines through a cholesterol-dependent mechanism. Planta Med 82: 1532-1539, 2016.
37. Fallahi M, Keyhanmanesh R, Khamaneh AM, Saadatlou MA, Saadat S and Ebrahimi H: Efect of alpha-hederin, the active constituent of Nigella sativa, on miRNA126, IL-13 mRNA levels and infammation of lungs in ovalbuminsensitized male rats. Avicenna J Phytomed 6: 77-85, 2016.
38. Keyhanmanesh R, Saadat S, Mohammadi M, Shahbazfar AA and Fallahi M: The protective efect of α-hederin, the active constituent of nigella sativa, on lung infammation and blood cytokines in ovalbumin sensitized guinea pigs. Phytother Res 29: 1761-1767, 2015.
39. Li J, Wu DD, Zhang JX, Wang J, Ma JJ, Hu X and Dong WG: Mitochondrial pathway mediated by reactive oxygen species involvement in α-hederin-induced apoptosis in hepatocellular carcinoma cells. World J Gastroenterol 24: 1901-1910, 2018.
40. Cheng L, Xia TS, Wang YF, Zhou W, Liang XQ, Xue JQ, Shi L, Wang Y, Ding Q and Wang M: The anticancer efect and mechanism of α-hederin on breast cancer cells. Int J Oncol 45: 757-763, 2014.